



Ultrahigh-charge electron beams from laser-irradiated solid surface

Yong Ma^{a,b}, Jiarui Zhao^a, Yifei Li^a, Dazhang Li^c, Liming Chen^{a,d,e,f,1}, Jianxun Liu^g, Stephen J. D. Dann^b, Yanyun Ma^{g,1}, Xiaohu Yang^g, Zheyi Ge^g, Zhengming Sheng^{d,e,h}, and Jie Zhang^{d,e,f,1}

^aInstitute of Physics, Chinese Academy of Sciences, Beijing 100190, China; ^bDepartment of Physics, Lancaster University, Bailrigg LA1 4YW, United Kingdom; ^cInstitute of High Energy Physics, Chinese Academy of Sciences, Beijing 100049, China; ^dCollaborative Innovation Center of Inertial Fusion Sciences and Applications, Shanghai Jiao Tong University, Shanghai 200240, China; ^eSchool of Physics and Astronomy, Shanghai Jiao Tong University, Shanghai 200240, China; ^fSchool of Physical Sciences, University of Chinese Academy of Sciences, Beijing 100049, China; ^gCollege of Science, National University of Defense Technology, Changsha 410073, China; and ^hDepartment of Physics, Scottish Universities Physics Alliance, University of Strathclyde, Glasgow G4 0NG, United Kingdom

Contributed by Jie Zhang, May 21, 2018 (sent for review January 29, 2018; reviewed by Sergei Bulanov and Yoshiaki Kato)

Compact acceleration of a tightly collimated relativistic electron beam with high charge from a laser–plasma interaction has many unique applications. However, currently the well-known schemes, including laser wakefield acceleration from gases and vacuum laser acceleration from solids, often produce electron beams either with low charge or with large divergence angles. In this work, we report the generation of highly collimated electron beams with a divergence angle of a few degrees, nonthermal spectra peaked at the megaelectronvolt level, and extremely high charge (~ 100 nC) via a powerful subpicosecond laser pulse interacting with a solid target in grazing incidence. Particle-in-cell simulations illustrate a direct laser acceleration scenario, in which the self-filamentation is triggered in a large-scale near-critical-density plasma and electron bunches are accelerated periodically and collimated by the ultraintense electromagnetic field. The energy density of such electron beams in high-Z materials reaches to $\sim 10^{12}$ J/m³, making it a promising tool to drive warm or even hot dense matter states.

laser–plasma interaction | direct laser acceleration | ultrahigh-charge beam | high energy density | near-critical-density plasma

In studies of laser–plasma acceleration (LPA), several laser wakefield accelerator (LWFA) (1) concepts have been proposed in the last few decades, including the plasma beat wave accelerator (1, 2), the self-modulated laser wakefield accelerator (SM-LWFA) (3), the cross-modulated laser wakefield accelerator (XM-LWFA) (4), and LWFA in the bubble regime (5, 6). The successful generation of high-quality electron beams at the gigaelectronvolt scale with quasi-monoenergetic spectra has stimulated the study of LPAs worldwide (7–14). However, almost all LPA experiments and theoretical models are based on interactions between lasers and gases, limiting the beam charge to typically a few tens of picocoulombs. While the charge of the electron bunch could reach a few nanocoulombs in laser–solid interactions due to higher absorption efficiency and attempts have been made to optimize beam collimation (15–23), the beam quality still needs to be greatly improved due to large divergence angles and quasi-thermal broad energy spectra. Such electrons are usually generated via several heating mechanisms such as resonant absorption (24, 25), vacuum heating (25–27), $J \times B$ heating (28), and stochastic heating (29). Directional electron beams with nanocoulomb charge have been produced via vacuum laser acceleration (VLA) with a plasma mirror injector (30). Unfortunately, the beam collimation also suffers from the ponderomotive force of the laser pulse in vacuum during acceleration, which results in a large divergence angle (hundreds of milliradians) and a halo in the electron beam profile. Recently, a few megaelectronvolts of quasi-monoenergetic electron acceleration have been observed in femtosecond laser–solid interaction with beam divergence angles of 1° – 2° (31). However, the beam charge is still limited to hundreds of

picocoulombs, and the underlying physics of such acceleration remain unclear.

In this work, electron beams with extremely high beam charge of approximately 100 nC are generated in 200-TW, subpicosecond laser–solid interactions with deliberately induced preplasma. The electron beams are highly collimated with an average divergence angle $< 3^\circ$ and the energy spectra are nonthermal with peaks at several megaelectronvolts. Particle-in-cell (PIC) simulations illustrate a scenario of electron acceleration in which the acceleration and confinement regimes are combined in a unique way. It is shown that electron beams are mainly produced via direct laser acceleration (DLA) (32–38) in plasma channels (39, 40) driven by the long laser pulse in a large-scale near-critical preplasma. The strong electromagnetic field inside the plasma channel confines the electron beams tightly. The significant improvement of the beam charge benefits from the persistent DLA process.

Experimental Results

The experiment was performed on Titan at the Jupiter Laser Facility at Lawrence Livermore National Laboratory (LLNL). The setup of the experiment is shown in Fig. 1. Copper block targets were irradiated by a 200-TW, subpicosecond laser at an incident angle of 72° in P polarization. The laser pedestal 3 ns

Significance

In the last three decades, the laser–plasma accelerator (LPA) has shown a rapid development owing to its super-high-accelerate gradients, which makes it a very promising compact accelerator and light source. Acceleration of a high-quality electron beam with divergence angle as small as possible and beam charge as high as possible has been a long-term goal ever since the inception of the LPA concept. However, until now the most popular acceleration scenario has failed to achieve both goals. We solved this problem and obtained tightly collimated electron beams with small divergence angle and extremely high beam charge (~ 100 nC) via the powerful ps laser pulse interacting with a solid target.

Author contributions: L.C. and J. Zhang designed research; Yong Ma, J. Zhao, Y.L., D.L., and L.C. performed research; Yong Ma, J.L., S.J.D.D., Yanyun Ma, X.Y., and Z.G. contributed new reagents/analytic tools; Yong Ma, J. Zhao, Y.L., and L.C. analyzed data; Yong Ma, L.C., and Z.S. wrote the paper; and J. Zhang facilitated the experiment and led the whole project.

Reviewers: S.B., Extreme Light Infrastructure-Beamlines; and Y.K., The Graduate School for the Creation of New Photonics Industries.

The authors declare no conflict of interest.

This open access article is distributed under [Creative Commons Attribution-NonCommercial-NoDerivatives License 4.0 \(CC BY-NC-ND\)](https://creativecommons.org/licenses/by-nc-nd/4.0/).

¹To whom correspondence may be addressed. Email: jzhang1@sjtu.edu.cn, lmchen@iphy.ac.cn, or yanyunma@126.com.

Published online June 18, 2018.

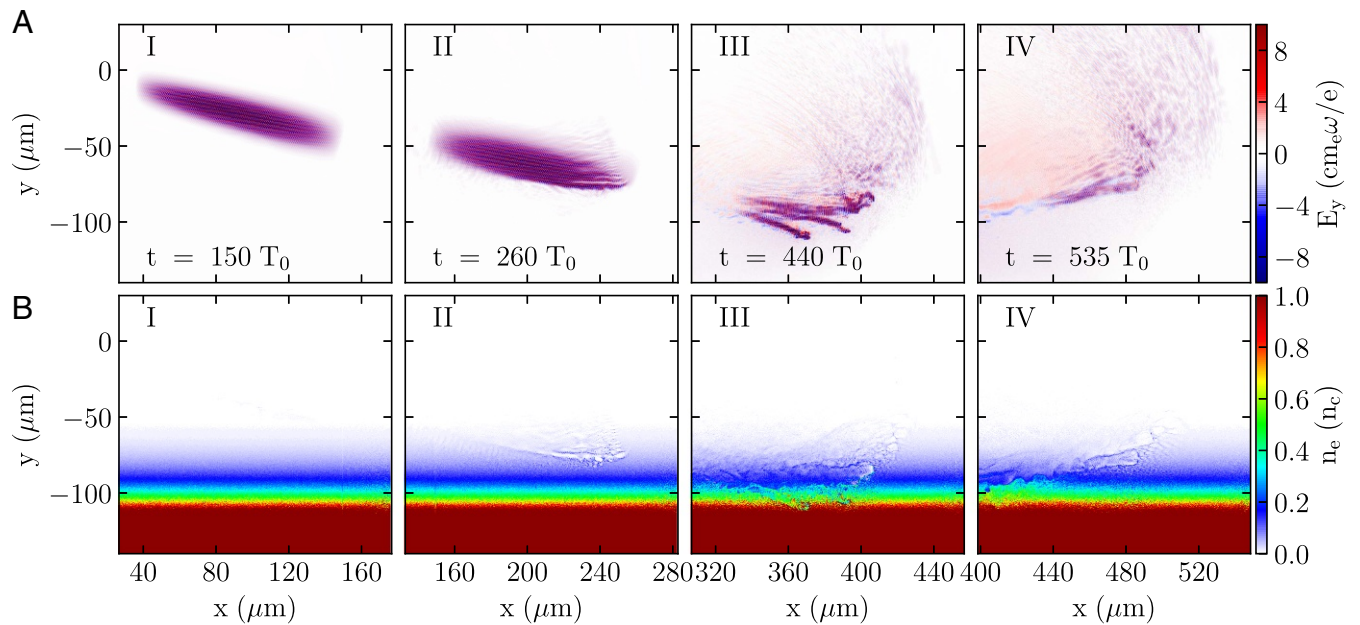


Fig. 5. Snapshots of laser fields and plasma electron density distributions at four time steps in PIC simulation. (A, I–IV) Laser field distributions. (B, I–IV) Plasma electron density distributions.

at a later stage. In Fig. 7, the vertical dashed line separates the electron trajectories into two parts. The right-hand side represents the DLA, while the left-hand side represents the stochastic heating. The stochastic motion of electrons in the laser field appears as abrupt “jumps” in electron trajectories (similar phenomena can be found in ref. 34), which act as a trigger to make the DLA happen. As deeply studied in ref. 29, efficient DLA can be triggered by stochastic motion of electrons when the laser fields exceed some threshold amplitudes, using two counterpropagating laser pulses. While in our work, the interference of the incident and reflected laser pulses results in

high-amplitude field and the enhanced stochastic motion eventually leads to the efficient DLA.

As a consequence of the collimation and acceleration inside the plasma channel, the electron spectrum agrees with that of the experiment, as shown in Fig. 6F. The simulated electron beam propagates along 22.1° from the x axis, close to the laser specular, with a FWHM divergence angle of 5.9° .

Our experimental observation can exclude another electron acceleration mechanism, VLA, in laser–solid interaction. In VLA, during the direct interaction with the laser field, electrons will escape the focal volume transversely after gaining

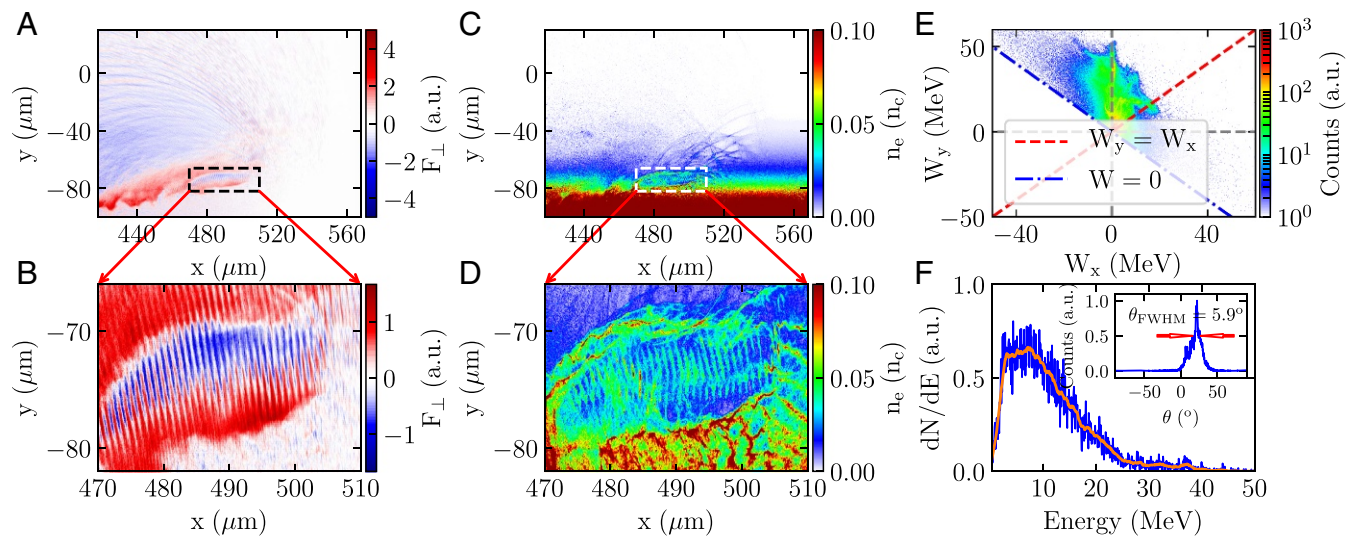


Fig. 6. (A and C) The transverse force and plasma density distribution at $t = 555 T_0$. (B and D) The transverse focusing force and the fine structure of the electron beam distribution inside a plasma channel. (E) The energy gain components distribution in (W_x, W_y) space at $t = 555 T_0$. The red dashed line divides the space into two regions: DLA-dominated region in the upper left and the wakefield acceleration-dominated region in the lower right. Electrons above the horizontal gray dashed line gain energy in the laser field while those below lose energy. Electrons to the right of the vertical dashed line gain energy from the wakefield while those to the left lose energy. (F) The energy spectrum of electrons escaping from the plasma at a slightly later time at $t = 585 T_0$. Inset shows the corresponding angular distribution of the electron beam.

Simulations. The simulations were performed using the PIC code EPOCH (53). The pulse duration of the incident laser is 270 fs (FWHM) with a spot size of 7 μm . The wavelength, incident angle, and polarization of the laser are the same as those in the experiment. The peak intensity of the laser is $2.8 \times 10^{20} \text{ W/cm}^2$.

The simulation box is initially located in $y \in (-140, 30) \mu\text{m}$ and $x \in (0, 150) \mu\text{m}$ with a moving window in x . The target plasma is located in $y \in (-140, -10) \mu\text{m}$ with density profile of $n_e = 10^{-(y+110)/25} n_c$ in y . The grid size is $\lambda_i/40$ in both directions and each cell contains 42 numerical macroparticles. The density profile is given by the radiation hydrodynamic code MULTI (54) by assuming the laser contrast is 10^{-6} .

The work done by the electric field can be split into x , y , and z :

$$W = -\frac{e}{m_e c^2} \int_0^t (E_x v_x) + (E_y v_y) + (E_z v_z) dt'. \quad [1]$$

The EPOCH code was modified to track these components (55):

- Tajima T, Dawson JM (1979) Laser electron accelerator. *Phys Rev Lett* 43:267–270.
- Rosenbluth MN, Liu CS (1972) Excitation of plasma waves by two laser beams. *Phys Rev Lett* 29:701–705.
- Krall J, Ting A, Esarey E, Sprangle P (1993) Enhanced acceleration in a self-modulated-laser wake-field accelerator. *Phys Rev E* 48:2157–2161.
- Sheng Z, Mima K, Sentoku Y, Nishihara K, Zhang J (2002) Generation of high-amplitude plasma waves for particle acceleration by cross-modulated laser wake fields. *Phys Plasmas* 9:3147–3153.
- Pukhov A, Meyer-ter Vehn J (2002) Laser wake field acceleration: The highly nonlinear broken-wave regime. *Appl Phys B* 74:355–361.
- Kostyukov I, Pukhov A, Kiselev S (2004) Phenomenological theory of laser-plasma interaction in ‘bubble’ regime. *Phys Plasmas* 11:5265–5264.
- Mangles S, et al. (2004) Monoenergetic beams of relativistic electrons from intense laser-plasma interactions. *Nature* 431:535–538.
- Geddes C, et al. (2004) High-quality electron beams from a laser wakefield accelerator using plasma-channel guiding. *Nature* 431:538–541.
- Faure J, et al. (2004) A laser-plasma accelerator producing monoenergetic electron beams. *Nature* 431:541–544.
- Leemans WP, et al. (2006) GeV electron beams from a centimetre-scale accelerator. *Nat Phys* 2:696–699.
- Hafz NAM, et al. (2008) Stable generation of GeV-class electron beams from self-guided laser-plasma channels. *Nat Photon* 2:571–577.
- Wang X, et al. (2013) Quasi-monoenergetic laser-plasma acceleration of electrons to 2 GeV. *Nat Commun* 4:1988.
- Kim HT, et al. (2013) Enhancement of electron energy to the multi-GeV regime by a dual-stage laser-wakefield accelerator pumped by petawatt laser pulses. *Phys Rev Lett* 111:165002.
- Leemans WP, et al. (2014) Multi-GeV electron beams from capillary-discharge-guided subpetawatt laser pulses in the self-trapping regime. *Phys Rev Lett* 113:245002.
- Chen LM, et al. (2001) Effects of laser polarization on jet emission of fast electrons in femtosecond-laser plasmas. *Phys Rev Lett* 87:225001.
- Li YT, et al. (2001) Hot electrons in the interaction of femtosecond laser pulses with foil targets at a moderate laser intensity. *Phys Rev E* 64:046407.
- Kodama R, et al. (2000) Long-scale jet formation with specularly reflected light in ultraintense laser-plasma interactions. *Phys Rev Lett* 84:674–677.
- Li YT, et al. (2006) Observation of a fast electron beam emitted along the surface of a target irradiated by intense femtosecond laser pulses. *Phys Rev Lett* 96:165003.
- Habara H, et al. (2006) Surface acceleration of fast electrons with relativistic self-focusing in preformed plasma. *Phys Rev Lett* 97:095004.
- Mordovanakis AG, et al. (2009) Quasimonoenergetic electron beams with relativistic energies and ultrashort duration from laser-solid interactions at 0.5 kHz. *Phys Rev Lett* 103:235001.
- Tian Y, et al. (2012) Electron emission at locked phases from the laser-driven surface plasma wave. *Phys Rev Lett* 109:115002.
- Mao JY, et al. (2012) Spectrally peaked electron beams produced via surface guiding and acceleration in femtosecond laser-solid interactions. *Phys Rev E* 85:025401.
- Wang W, et al. (2013) Collimated quasi-monoenergetic electron beam generation from intense laser solid interaction. *High Energy Density Phys* 9:578–582.
- Estabrook K, Kruger WL (1978) Properties of resonantly heated electron distributions. *Phys Rev Lett* 40:42–45.
- Bulanov SV, Naumova NM, Pegoraro F (1994) Interaction of an ultrashort, relativistically strong laser pulse with an overdense plasma. *Phys Plasmas* 1:745–757.
- Brunel F (1987) Not-so-resonant, resonant absorption. *Phys Rev Lett* 59:52–55.
- Chen L, et al. (2001) Hot electron generation via vacuum heating process in femtosecond laser-solid interactions. *Phys Plasmas* 8:2925–2929.
- Kruer W, Estabrook K (1985) JxB heating by very intense laser-light. *Phys Fluids* 28:430–432.
- Sheng ZM, et al. (2002) Stochastic heating and acceleration of electrons in colliding laser fields in plasma. *Phys Rev Lett* 88:055004.
- Thevenet M, et al. (2016) Vacuum laser acceleration of relativistic electrons using plasma mirror injectors. *Nat Phys* 12:355–360.
- Mao JY, et al. (2015) Highly collimated monoenergetic target-surface electron acceleration in near-critical-density plasmas. *Appl Phys Lett* 106:131105.
- Pukhov A, Sheng ZM, ter Vehn JM (1999) Particle acceleration in relativistic laser channels. *Phys Plasmas* 6:2847–2854.
- Gahn C, et al. (1999) Multi-MeV electron beam generation by direct laser acceleration in high-density plasma channels. *Phys Rev Lett* 83:4772–4775.
- Mangles SPD, et al. (2005) Electron acceleration in cavitated channels formed by a petawatt laser in low-density plasma. *Phys Rev Lett* 94:245001.
- Kneip S, et al. (2008) Observation of synchrotron radiation from electrons accelerated in a petawatt-laser-generated plasma cavity. *Phys Rev Lett* 100:105006.
- Li YY, et al. (2011) Direct laser acceleration of electron by an ultra intense and short-pulsed laser in under-dense plasma. *Phys Plasmas* 18:053104.
- Zhang X, Khudik VN, Shvets G (2015) Synergistic laser-wakefield and direct-laser acceleration in the plasma-bubble regime. *Phys Rev Lett* 114:184801.
- Huang TW, et al. (2016) Characteristics of betatron radiation from direct-laser-accelerated electrons. *Phys Rev E* 93:063203.
- Willingale L, et al. (2011) High-power, kilojoule class laser channeling in millimeter-scale underdense plasma. *Phys Rev Lett* 106:105002.
- Willingale L, et al. (2013) Surface waves and electron acceleration from high-power, kilojoule-class laser interactions with underdense plasma. *New J Phys* 15:025023.
- Alfvén H (1939) On the motion of cosmic rays in interstellar space. *Phys Rev* 55:425–429.
- Dodin IY, Fisch NJ (2006) Correction to the Alfvén-Lawson criterion for relativistic electron beams. *Phys Plasmas* 13:103104.
- Sentoku Y, et al. (1999) Plasma jet formation and magnetic-field generation in the intense laser plasma under oblique incidence. *Phys Plasmas* 6:2855–2861.
- Liu B, et al. (2013) Generating overcritical dense relativistic electron beams via self-matching resonance acceleration. *Phys Rev Lett* 110:045002.
- Kruer WL (1988) *The Physics of Laser Plasma Interactions* (Addison-Wesley, Redwood City, CA).
- Tzoufras M, et al. (2008) Beam loading in the nonlinear regime of plasma-based acceleration. *Phys Rev Lett* 101:145002.
- Bostedt C, et al. (2016) Linac coherent light source: The first five years. *Rev Mod Phys* 88:015007.
- Mitri SD, Cornacchia M (2014) Electron beam brightness in Linac drivers for free-electron-lasers. *Phys Rep* 539:1–48.
- Tabak M, et al. (1994) Ignition and high-gain with ultrapowerful lasers. *Phys Plasmas* 1:1626–1634.
- Tanaka KA, et al. (2005) Calibration of imaging plate for high energy electron spectrometer. *Rev Scientific Instr* 76:013507.
- Briesmeister JF (2000) MCNP: A general Monte Carlo N-Particle transport code. (Los Alamos National Laboratory, Los Alamos, NM), Technical Report LA-13709-M.
- Maddox BR, et al. (2011) High-energy x-ray backlighter spectrum measurements using calibrated image plates. *Rev Scientific Instr* 82:023111.
- Arber TD, et al. (2015) Contemporary particle-in-cell approach to laser-plasma modelling. *Plasma Phys Controlled Fusion* 57:1–26.
- Ramis R, ter Vehn JM, Ramirez J (2009) {MULTI2D}—A computer code for two-dimensional radiation hydrodynamics. *Computer Phys Commun* 180:977–994.
- Shaw JL, et al. (2017) Role of direct laser acceleration of electrons in a laser wakefield accelerator with ionization injection. *Phys Rev Lett* 118:064801.